Alpha-synuclein Oligomers Distinctively Permeabilize Complex Model Membranes*

Anja N.D. Stefanovic[1], Martin T. Stöckl[1,2], Mireille M. A. E. Claessens[1], Vinod Subramaniam[1,3]

[1] Nanobiophysics group, MIRA Institute for Biomedical Technology and Technical Medicine and MESA+ Institute for Nanotechnology, University of Twente, PO Box 217, 7500AE, The Netherlands

[2] present address: Bioimaging Center, University Konstanz, PO Box 604, Universitätsstraße 10, 78457 Konstanz, Germany

[3] present address: FOM Institute AMOLF, Science Park 104, 1098XG Amsterdam, The Netherlands

Running title: α-synuclein oligomer-complex membrane interactions

Correspondence: Vinod Subramaniam, FOM Institute AMOLF, Science Park 104, 1098 XG Amsterdam, The Netherlands, Tel.: +31 20 7547100; Fax: +31 20 754 7290; Email: subramaniam@amolf.nl

Key words: Alpha-synuclein; cardiolipin; model membranes; oligomers; permeabilization

Alpha-synuclein oligomers are increasingly considered to be responsible for the death of dopaminergic neurons in Parkinson's disease. The toxicity mechanism of alpha-synuclein oligomers likely involves membrane permeabilization. Even though it is well established that alpha-synuclein oligomers bind and permeabilize vesicles composed of negatively charged lipids, little attention has been given to the interaction of oligomers with bilayers of physiologically relevant lipid compositions. We investigated the interaction of alpha-synuclein with bilayers composed of lipid mixtures that mimic the composition of plasma and mitochondrial membranes. Here we show that monomeric and oligomeric alpha-synuclein bind to these membranes. The resulting membrane leakage differs from what is observed for simple artificial model bilayers. While the addition of oligomers to negatively charged lipid vesicles displays fast content release in a bulk permeabilization assay, adding oligomers to vesicles with compositions mimicking mitochondrial membranes shows a much slower loss of content. Oligomers are not able to induce leakage in the artificial plasma membranes even after long-term incubation. Circular dichroism experiments indicate that binding to lipid bilayers initially induces conformational changes in both oligomeric and monomeric alpha-synuclein, that show little change upon long-term incubation of oligomers with membranes. Our results show that the mitochondrial model membranes are more vulnerable to permeabilization by oligomers than model plasma membranes reconstituted from brain-derived lipids; this preference may imply that increasingly complex membrane components, such as those in the plasma membrane mimic used here, are less vulnerable to damage by oligomers.

Introduction

Parkinson's disease (PD) is one of the most common human neurodegenerative diseases, involving the progressive loss of dopaminergic neurons in the *substantia nigra* in the midbrain [1]. The appearance of Lewy bodies (LB) is characteristic of the pathology of PD. The main component of these LBs is the protein alpha-synuclein (αS), which is present as amyloid fibrils. αS is a 140 amino acid intrinsically disordered protein [2-7] of as yet unknown function. In PD, aggregation of αS causes the protein to lose its putative function and gain toxicity [8-11]. αS consists of a positively charged N-terminal region (residues 1-60) containing imperfect KTKEGV repeats, a hydrophobic NAC region (residues 61-95) and a negatively charged C-terminal region (residues 96-140). For membrane binding the N-

terminal part of αS plays a key role. Upon binding to phospholipid membranes the protein adopts an α-helical structure [12, 13]. Interactions of monomeric αS with lipid vesicles of different compositions and size have been studied [14-19]. Current thinking suggests that intermediate species in the fibril formation pathway of αS are the toxic species involved in cell death in PD [10, 20-22]. In spite of structural differences between αS oligomers and monomers, they both show high affinity for negatively charged membranes. We have previously shown that oligomer binding induces leakage of artificial negatively charged lipid vesicles. Although several studies [23-25] have shown that isolated oligomers can decrease the integrity of simple negatively charged lipid vesicles, little is known on how these species bind and permeabilize natural membranes. Mitochondrial damage has been observed in PD and mitochondrial membranes are therefore thought to be a likely target for oligomer-induced damage [26-28]. Mitochondrial membranes are enriched in cardiolipin [29], a unique negatively charged diphosphatidylglycerol lipid. Monomeric αS shows a high binding affinity to cardiolipin-containing membranes [30, 31]. Quantitative correlation between αS in mitochondria and cytosol confirmed that monomeric αS interacts with mitochondrial membranes [32]. Moreover, it has been reported that αS is present on mitochondrial membranes in functional dopaminergic neurons of the *substantia nigra* [33, 34], where at physiological concentrations αS is mainly localized at the mitochondrial inner membrane and only a small fraction is found at the outer membrane [32, 35]. However, a contrasting report suggests αS is localized in the outer mitochondrial membrane [27]. Mitochondria of dopaminergic neurons in brains of PD patients contain a higher concentration of αS than normal brains [36]. A recent study has suggested that WT αS is mainly localized in mitochondria-associated endoplasmic reticulum (ER) membranes and modulates the morphology of mitochondria [37]. Besides these membranes, the plasma membrane has been indicated as a site of oligomer-induced damage. Upon internalization, αS colocalizes with the inner leaflet of the plasma membrane [38, 39]. In a yeast model it was found that αS binds to plasma membranes [40]. Finally, a recent report suggests that αS can interact with lipids in the plasma membrane increasing the membrane permeability as a potential mechanism of extracellular neurotoxicity [41].

Here we study the binding of specific, well-characterized, oligomeric αS species to lipid membranes made of physiologically relevant mitochondrial and plasma membrane lipid mixtures. We show that these oligomers cause slow permeabilization of mitochondrial inner membrane mimics, whereas they bind to, but could not induce leakage in, plasma membrane inner leaflet model systems.

Results

Binding of αS monomers to bilayers that mimic lipid composition of natural membranes

Electrostatic interactions play a key role in binding of monomers to negatively charged membranes. Membrane binding of monomers is mainly associated with positive charges on the N-terminal part of the protein [19]. Upon binding to negatively charged lipid bilayers, monomers adopt an amphipathic α-helical structure. Fluorescently labeled monomers colocalize with the control DOPG vesicles (**Figure 1A**) and with GUVs composed of both the plasma and mitochondrial membrane mimicking lipid mixtures (**Figure 1B** and **1C**). Analysis of the Alexa 488-fluorescence intensity at GUV membranes showed that the highest amount of monomers was bound at DOPG membranes (**Figure 1D**). Surprisingly not all brain PS:brain PE:ch vesicles bound monomers, with ~ 50% of the vesicles not showing any colocalization of labeled monomers and GUVs. It should be noted that in **Figure 1D** only vesicles that bind αS were taken into account.

CD spectroscopy was used to assess whether binding of monomers to vesicles of all lipid compositions resulted in conformational changes in the protein. Monomers in solution showed CD spectra typical for an intrinsically disordered protein with a negative peak at 198 nm. As previously reported, α-synuclein monomers form an α-helix upon binding to SUVs [13, 42]. Upon binding membranes mimicking plasma or mitochondrial lipid compositions, monomers adopt an α-helical structure that is characterized by two negative bands at 208 and 222 nm in the CD spectrum. The α-helical content of the protein upon binding was estimated from the MRE at 222 nm as explained in the Materials and Methods

section below. Binding of monomers to control DOPG vesicles resulted in an α-helical content of 65.1±1.2 %. Monomers binding to CL:POPE:POPC membranes or membranes composed of brain PS:brain PE:cholesterol adopted a comparable amount of α-helix (59.0±0.4 % and 61.1±0.3 % respectively) (**Figure 2**). The similarity of the CD spectra suggests that αS monomers were fully bound and in a predominantly α-helical conformation at saturating lipid concentrations for all types of natural membranes tested. There were no changes in α-helical content of αS monomers bound to brain PS:brain PE:ch vesicles when comparing CD spectra immediately after binding or after 20h of incubation (**Figure 2A**). CD data points below 205 nm were not taken into account because of the high noise, likely due to a presence of some other organic compounds in the lipid mixtures of brain lipids.

Do αS oligomers bind to bilayers mimicking the lipid composition of natural membranes and does this binding result in conformational changes?

We have previously shown that αS oligomers can bind to lipid membranes composed of negatively charged lipids such as DOPG or POPG [43]. The binding of fluorescently labeled oligomers to GUVs with a lipid composition mimicking either negatively charged, neuronal or mitochondrial membranes was studied using confocal microscopy. We observed that oligomers bind to bilayers mimicking the lipid composition of both the plasma membrane inner leaflet and the mitochondrial inner membrane (**Figure 3B** and **3C**). Semi-quantitative comparison of oligomer membrane binding was done in the same manner as for monomers. Oligomers showed comparable binding to DOPG, CL:POPE:POPC and brain PS:brain PE:ch GUVs (**Figure 3D**). As for monomer binding, we also observed that not all brain PS:brain PE:ch membranes bound oligomers.

We further investigated if the membrane binding caused conformational changes in the oligomers similar to those observed for monomeric αS using CD spectroscopy. In solution, oligomers showed some β-sheet conformation (**Figure 4**). Binding of oligomers to vesicles resulted in a small change in protein conformation for both lipid mixtures. Oligomers showed an increase in α-helical content upon addition of SUVs. The α-helical content of the oligomers was comparable for all lipid membranes studied, and did not change in time. Oligomers bound to brain PS:brain PE:cholesterol membranes showed similar CD spectra immediately after the addition of protein to membranes and after 20h of incubation (**Figure 4**). We investigated the membrane disrupting properties of oligomers by studying the kinetics of membrane permeabilization using a dye release assay.

Kinetics of membrane permeabilization (Dye release assay)

Oligomers have been shown to disrupt membranes composed of negatively charged lipid vesicles [23]. After the addition of oligomers to a solution of calcein-filled DOPG LUVs a rapid release of encapsulated dye was observed (**Figure 5A**). We have previously shown that monomers and fibrils also could cause membrane permeabilization of negatively charged PG vesicles, but that much higher concentrations of the protein are necessary to get comparable leakage [23]. Comparing the oligomer-induced leakage kinetics of the dye from DOPG LUVs with dye encapsulated in vesicles of lipid bilayers that mimic physiologically relevant membrane compositions revealed large differences. Although oligomer binding was observed after 30 minutes of incubation, little oligomer-induced vesicle leakage of membranes that mimic natural membranes was observed at these timescales. For LUVs composed of a mixture of CL:POPE:POPC a slow dye leakage was observed which was still increasing after 18h (**Figure 5B**). For these LUVs the oligomer-induced leakage was concentration dependent; higher oligomer concentrations showed more leakage. In contrast, even after 18 hour incubation, oligomer concentrations as high as 4 μM did not result in more than 2% membrane leakage for bilayers composed of brain PS:brain PE:cholesterol (**Figure 5C**). To obtain a better understanding of the observed slow release kinetics, we used the diffusion equation assuming steady state release to fit the data. In the absence of oligomers the change in concentration, *c*, of dye in the vesicles was assumed to follow the expression $c = c(0)(1 - e^{(-kt)})$ where the rate constant $k = P_C \times A/V$, V is the volume of the vesicle, P_c the membrane permeability for calcein

and A the area over which diffusion takes place. To fit the data in presence of oligomers, we expect the rate constant to change or more exponents to be required to better describe the dye release kinetics.

When oligomers were added, fast leakage was observed for DOPG LUVs. This is not the case for membranes composed of CL:POPE:POPC. Oligomer-induced leakage from these vesicles required a fit with at least three exponentials. One of these exponents is comparable for all oligomer concentrations (the exponent associated with amplitude C in **Table 1**). This amplitude (C) decreases with increasing oligomer concentration and was attributed to the calcein permeability of the bare bilayer. With increasing oligomer concentration a decreasing fraction of vesicles is not affected by oligomers and show leakage comparable to bare membranes. From the slow exponent attributed to the bare membrane, the calcein permeability P_c of the CL:POPE:POPC membrane was calculated to be $\sim 10^{-13}$ cm/s. The amplitudes of the other two exponents increase with increasing oligomer concentration indicating that these contributions result from the presence of oligomers. Both oligomer-related rate constants were observed to increase with increasing oligomer concentration (**Table 1**).

Discussion

It is well established that binding of αS to lipid bilayers is accompanied by an increase in α-helical content [13]. The binding of αS to lipid bilayers strongly depends on the presence of negatively charged lipids [13, 14, 19, 44-46]. However although most reports suggest that neutral membranes do not bind αS [13, 47], others claim differently [14, 48]. The amount of αS bound to lipid bilayers is proportional to the number of available binding sites and therefore to the fraction of negatively charged lipids in the bilayer [14, 19]. Earlier studies with brain derived lipids showed no binding of αS to lipid bilayers that contained only 10-15% of PS lipids indicating that the 20% used in our experiments is close to the minimal amount required for αS binding [13]. Variations in composition of the brain PS:brain PE:ch GUVs may explain why monomers did not bind to all brain PS:brain PE:ch GUVs. This variation in composition is possibly caused by the presence of brain PS in the lipid mixture. It has been claimed that brain PS can interfere with the electroformation of GUVs resulting in variation in lipid composition of the resulting vesicles [49].

In the presence of excess vesicles of all lipid compositions (DOPG or natural lipids), αS showed comparable results in CD binding studies. The maximal α-helical content of the protein did not depend on the negatively charged lipid species. Interactions of CL containing vesicles with αS monomers have been characterized by ^{19}F-NMR [31]. It was proposed that the positively charged N-terminal region is involved in binding via interaction between positively charged lysines and negatively charged CL [31]. The protein binds to lipid surfaces through an amphipathic α-helix adopted by 100 amino acid residues on the N-terminal part of the protein, while the acidic C-terminal tail of the protein remains in solution [2]. According to the literature, αS monomers adopt 41% α-helix in the presence of 1 mM of SDS [50], while upon the binding to DPPC:DPPG vesicles 61% of the protein adopted α-helical conformation [51], which is comparable to our observations.

Like αS monomers, oligomers were found to bind lipid bilayers of all compositions studied. However, compared to observations on αS monomers, the helical content observed in the presence of oligomers was much lower [23]. It is possible that only the monomers in the oligomer facing the bilayer bind the membrane and adopt an α-helical conformation. Alternatively, the interactions between αS monomers in the oligomer may be too strong to permit further conformational changes upon lipid binding.

Oligomers interacting with simple negatively charged lipid bilayers composed of e.g. DOPG or POPG immediately permeabilize these lipid membranes [25]. Fast content release was also observed for vesicles containing POPC:DOPA lipids [23, 43]. The binding of oligomers to lipid bilayers has been reported to not always result in membrane permeabilization [23, 25]. Even 30 minutes after addition of the oligomers POPG:POPC bilayers remained intact [43, 52]. For the two component lipid mixture CL:POPC (1:3), a lipid composition that comes close to that of mitochondrial membranes, no leakage was observed at short time scales [23]. Here we show that interaction of oligomers with bilayers does not necessarily result in a fast loss of membrane integrity. Membranes with a lipid composition

(CL:POPE:POPC (4:3:5)) similar to that reported earlier [23] show some dye release over 18 hours (**Figure 5B**). However, even on these long time scales oligomer binding did not result in permeabilization of the plasma membrane mimicking lipid bilayers (brain PS:brain PE:cholesterol) (**Figure 5C**). To describe the oligomer-induced calcein release kinetics from CL:POPE:POPC vesicles at least three exponentials, and therefore at least three rate constants, were necessary. The presence of more than one rate constant suggests that subpopulations of vesicles are differently affected by the addition of oligomers. The value of one of the rate constants (k_3 in **Table 1**) describing the calcein flux as a function of oligomer concentration is comparable to that observed for lipid bilayers in the absence of oligomers [53, 54]. This suggests that a fraction of the vesicles is not affected by the oligomers. Oligomers either did not bind or did not affect the calcein permeability of this fraction. As expected, the fraction of unaffected vesicles becomes smaller with increasing oligomer concentration. The amplitude of the other two exponents increases with the oligomer concentration. The dye release kinetics described by these two exponents is therefore attributed to the presence of oligomers in or on the lipid bilayer. Surprisingly both rate constants are observed to increase with increasing oligomer concentrations (See **Table 1**). The oligomer-dependent exponents are expected to contain contributions of both the lipid bilayer and the oligomers. Because the leakage is much faster in the presence of oligomers we assume that the contribution of oligomers is very large compared to the contribution of the bare bilayer. As indicated in the Results section the value of *k* does not only depend on the permeability coefficient *P* but also on the volume of the vesicle and the area over which diffusion takes place. With increasing oligomer concentrations, the area covered by oligomers is expected to become larger. In contrast to our observation this increase in oligomer area should give rise to an increase in the rate constants contributed to oligomers. The observed decrease in the rate constants may result from an increase in vesicle volume, i.e. by incorporation of oligomers in the lipid bilayer. Dynamic light scattering experiments indicate that CL:POPE:POPC LUVs indeed become larger upon incubation with oligomers supporting the hypothesis that the decrease in rate constants corresponding to oligomer-induced leakage results from a volume increase. The observed change in CL:POPE:POPC vesicles diameter of approximately 30 nm corresponds to the expected volume change resulting from oligomer incorporation (**Figure 6**). The decrease in leakage observed for brainPS:brainPE:CH bilayers in the presence of oligomers possibly results from the binding of oligomers and blocking of the membrane surface. The permeability of the oligomer-covered surface is low compared to the permeability of the bare membrane surface.

Recent data on more physiologically relevant Brain Total Lipid Extract membranes (BTLEM) have shown that αS causes bilayer defects [55]. We speculate that the brain PS: brain PE:ch model system we use may show lipid rearrangement similar to that proposed for BTLEM membranes. Cholesterol in complex model brain PS:brain PE:ch membranes can have an additional stabilizing effect on these membranes [23, 43, 48, 56] making them less vulnerable to oligomer-induced leakage. In our experimental system, the inclusion of cholesterol at constant charge density does not appear to have any appreciable effect of the extent of permeabilization (**Figure 7**). However, it has been suggested that the amount of cholesterol in the plasma membrane is important for formation of amyloid channels [57, 58].

For the amyloid forming protein Islet Amyloid Polypeptide, slow dye release from POPG:POPC vesicles was concluded to be caused by the formation of fibrils [59]. The experiments presented here were performed with stable oligomers [60]. We thus do not expect that conformational changes and further aggregation play a role in long-term leakage kinetics. Alternatively any conformational changes in the oligomer may be beyond our detection limit because they involve only a few proteins.

The membrane leakage data presented suggest that complex lipid membranes are less prone to oligomer-induced damage. The complexity of model plasma membranes lies in the composition of the membranes itself, consisting largely of combinations of long and polyunsaturated lipids in the brain lipid extracts used. Our results show that mitochondrial model membranes are more prone to oligomer-induced damage at longer timescales

while the more complex plasma membrane model systems do not show a concentration dependent permeabilization on the same time scale. Other *in vitro* studies have suggested that the mitochondria specific lipid CL is essential for αS mitochondrial membrane interactions [46]. A recent study [61] confirmed a common mechanism of damage of mitochondrial membranes by amyloid induced species via direct interactions of these species with membrane phospholipids. Their proposed mechanism agrees very well with our data on mitochondrial model membranes, which is mediated by increased affinity of these species for CL.

Materials and methods

Expression and purification of αS

Expression and purification of human wild-type (wt) αS and the cysteine (cys) mutant αS-A140C, where alanine at position 140 was replaced with a cysteine, was done as previously described [62]. The protein concentration was determined by measuring the absorbance on a Shimadzu spectrophotometer at 276 nm, using molar extinction coefficients of 5600 $M^{-1}cm^{-1}$ for wt and 5745 $M^{-1}cm^{-1}$ for A140C [60, 63]. The protein was stored at -80°C until further use.

Labeling of αS

The cys mutant αS-A140C was used for labeling the protein with an Alexa Fluor 488 C5 maleimide dye (A488). Prior to labeling, a six-fold molar excess of dithiothreitol (DTT) was added to αS-A140C to reduce disulfide bonds. After 30 minutes of incubation, DTT was removed using Zeba Spin desalting columns, and a two-fold excess of A488 was added. After 1 hour incubation, excess of free dye was removed using two desalting steps. The labeling efficiency was estimated to be between 90-100% from absorption spectra. To determine the protein and A488 concentration the absorbance at 276 nm was measured using a molar extinction coefficient of 5745 M^{-1} cm^{-1} for the protein and at 495 nm using a molar extinction coefficient of 72000 M^{-1} cm^{-1} for the dye.

Preparation of unlabeled and labeled αS oligomers

Briefly, oligomers were obtained by incubating αS at high concentrations in the absence of additional factors [23]. Alexa 488 labeled oligomers with 7.5 % labeling density, achieved by mixing appropriate quantities of labeled protein (αS-A140C) with unlabeled protein (WT), were prepared for membrane binding studies by confocal microscopy. Oligomers were purified and separated from monomers using size-exclusion chromatography on a Superdex^{TM} 200 10/300 GL column (GE Healthcare Bio-Sciences AB, Uppsala, Sweden). Separation of oligomers from monomers is based on size, where larger particles (oligomers) elute first. To confirm the presence of oligomers a native PAGE gradient gel was used [23] with a polyacrylamide gradient between 3 and 16%. We have previously demonstrated that oligomers prepared in this manner are composed of ~ 30 monomers, and are stable [60]. Monomers could not be detected in the oligomer preparation (data not shown).

LUVs preparation and calcein release assay

All lipids were purchased from Avanti Polar Lipids (Alabaster, AL). In the experiments the following lipids were used: 1-Palmitoyl-2-oleoylphosphatidylcholine (POPC), 1,2-dioleoylphosphatidylglycerol (DOPG), 1-Palmitoyl-2-oleoylphosphatidylethanolamine (POPE), 1',3'-bis[1,2-dioleoyl-sn-glycero-3-phospho]-sn-glycerol (18:1 Cardiolipin, CL), porcine brain L-α-phosphatidylserine (Brain PS), porcine brain L-α-phosphatidylethanolamine (Brain PE) and cholesterol (ch).

To mimic the lipid composition of neuronal plasma membranes we used mixtures of brain PS:brain PE:cholesterol in a molar ratio of 2:5:3, which corresponds to 20% of negatively charged lipids. However, no elaborative data of brain lipid composition are available. The neuronal membrane has approximately 10% negatively charged lipids, mainly PS, while the main components of these membranes are neutral PC and PE phospholipids [64]. However, this estimation of the lipid composition does not take into account asymmetry between the inner and outer leaflets of the membrane [13]. Because αS is an intracellular protein, we chose to the mimic the inner leaflet of the plasma membrane, which is enriched in PS. αS has also been implicated in interactions with mitochondrial membranes. Literature data suggests that αS preferentially binds to the mitochondrial inner membrane [29]. To mimic the mitochondrial inner membrane we used a lipid composition that contains CL:POPE:POPC in a molar ratio 4:3:5 [29].

Specific lipid compositions were prepared by mixing 650 µM of lipids in chloroform. The solvent was removed by drying under nitrogen flow. The resulting lipid films were then hydrated for 1 hour using 50 mM calcein, 10 mM HEPES (4-(2-Hydroxyethyl)piperazine-1-ethanesulfonic acid), 60 mM NaCl to obtain an osmolality (Cryoscopic osmometer, Gonotec) of 320 mOsm/kg. The sample was then subjected to 5 freeze-thaw cycles using liquid nitrogen and a water bath. The temperature of the water bath was kept above the transition temperature of the lipid mixture. The solution was subsequently extruded 11 times through 100 nm pore size filters (Whatman) and finally unencapsulated calcein was removed using PD-10 columns filled with Sephadex G-100 (GE Healthcare).

Long-term calcein release kinetics of the model membranes was followed on a Varian Cary Eclipse fluorometer. We used lipid concentrations of 40 µM. The emission intensity was recorded at 515 nm for excitation at 495 nm. TritonX (0.5%) was added to completely lyse the vesicles. All the data points were normalized using the intensity after TritonX treatment as 100 % leakage.

Semi-quantitative αS monomer and oligomer binding assay

Giant unilamellar vesicles (GUVs) were prepared in sucrose solution as previously described by Angelova [65]. The sucrose concentration was equiosmolar to the 10mM HEPES, 150mM NaCl solution in which the proteins were dissolved. 1% DOPE-Rhodamine was included in the previously mentioned lipid mixtures to facilitate visualization of the lipid membrane.

GUVs mimicking natural lipid compositions were equilibrated with fluorescently labeled oligomers for 30 minutes before imaging. DOPG vesicles were used as a positive control for binding of monomers and oligomers to membranes.

Our experiments were performed using the same experimental settings (master gain, digital offset and laser power) for imaging the binding of both monomers (Figure 1) and oligomers (Figure 3). DOPE-Rhodamine was excited with a He/Ne laser (543 nm) and Alexa 488 was excited with an Argon laser (488 nm) on a Zeiss CLSM 510 confocal microscope. We used the ImageJ script plot profile to extract semi-quantitative fluorescence values reporting on the binding of monomers and oligomers to membranes. The amount of αS bound to GUV membranes was estimated from the peak values of the Alexa 488 intensity profiles and averaged for at least 15 vesicles on five random cross sections using the same imaging settings (master gain, digital offset and laser power). Figures 1A, 1B, 1C and 3A, 3B and 3C are representative confocal images of the binding of fluorescently labeled alpha-synuclein monomers (Figure 1) and oligomers (Figure 3).

SUVs preparation and binding of αS oligomers to SUVs

Lipid mixtures that contain 3.8 mM of lipids in chloroform were prepared. After removing traces of chloroform a thin lipid film was dissolved in 10 mM K-phosphate buffer. SUVs were prepared from this solution by sonicating for half an hour using a tip sonicator (Labsonic) at maximum amplitude on ice. Binding-induced conformational changes of oligomeric and monomeric alpha-synuclein were investigated using CD spectroscopy [66]. Both protein and lipids samples were prepared in 10 mM K-phosphate buffer. Spectra were recorded in Jasco 715 spectropolarimeter from 190 to 260 nm with a step size of 0.2 nm, band width 2 nm, scanning speed 50 nm/min in 1 mm quartz cuvettes. The spectra represent averages of three scans and were corrected for the background from K-phosphate buffer and αS-free vesicles. Monomer and oligomer concentrations were 16 µM and 10 µM of equivalent monomer concentration respectively, keeping the lipid to protein ratio 260:1 for oligomer binding to SUVs and 170:1 for monomers binding to SUVs. A lipid concentration of 2.72 mM gave us the above-mentioned lipid to protein ratio. These ratios were chosen to obtain complete binding of the protein [13, 42]. Mean residue ellipticities (MRE, deg $dmol^{-1}$ cm^2) were calculated using Equation 1, where c is the protein concentration, l is the pathlength cuvette and $n_{residues}$ is the number of residues (amino acids).

$$MRE = \frac{recorded\ value - buffer\ value}{l(cm) \times n_{residues} \times 10 \times c(M)} \quad (1)$$

In principle the MRE at any wavelength is a combination of α-helical structure, β-sheet and random coil content of the sample [67]. The α-helical content was estimated by measuring the CD signal at 222 nm; at this wavelength the contribution of random coil structure is relatively small [68].

At 222 nm the α-helical content was obtained using Equations 2-4:

$$\%helicity = \frac{\theta_{222} - \theta_{coil}}{\theta_{helix} - \theta_{coil}} \times 100 \quad (2)$$

where θ_{helix} and θ_{coil} could be calculated:

$$\theta_{coil} = 640 - 45 \times \vartheta \quad (3)$$

$$\theta_{helix} = -40000 \times \left(1 - \frac{2.5}{n}\right) + 100 \times \vartheta \quad (4)$$

Θ_{222} is the measured mean residue ellipticity at 222 nm, θ_{helix} and θ_{coil} are mean residue ellipticities at 222 nm of idealized α-helix and random coil proteins, n=140 amino acids, and ϑ is temperature in ^{o}C.

Acknowledgments

We thank Kirsten van Leijenhorst-Groener and Nathalie Schilderink for assistance in expression and purification of alpha-synuclein. This work was financially supported by the "Nederlandse Organisatie voor Wetenschappelijk Onderzoek" (NWO) through the NWO-CW TOP grant number 700.58.302.

Author Contributions

A.N.D.S. planned and performed the experiments, and analyzed the data. All authors contributed to interpreting the data and writing the manuscript.

References

1. Cookson, M. R. (2009) alpha-Synuclein and neuronal cell death, *Mol Neurodegener.* **4**, 9.
2. Eliezer, D., Kutluay, E., Bussell, R., Jr. & Browne, G. (2001) Conformational properties of alpha-synuclein in its free and lipid-associated states, *J Mol Biol.* **307**, 1061-73.
3. Uversky, V. N., Li, J. & Fink, A. L. (2001) Evidence for a partially folded intermediate in alpha-synuclein fibril formation, *J Biol Chem.* **276**, 10737-44.
4. Lorenzen, N., Nielsen, S. B., Buell, A. K., Kaspersen, J. D., Arosio, P., Vad, B. S., Paslawski, W., Christiansen, G., Valnickova-Hansen, Z., Andreasen, M., Enghild, J. J., Pedersen, J. S., Dobson, C. M., Knowles, T. P. J. & Otzen, D. E. (2014) The role of stable α-synuclein oligomers in the molecular events underlying amyloid formation, *J Am Chem Soc*.
5. Roche, J., Ying, J. F., Maltsev, A. S. & Bax, A. (2013) Impact of Hydrostatic Pressure on an Intrinsically Disordered Protein: A High-Pressure NMR Study of alpha-Synuclein, *Chembiochem.* **14**, 1754-1761.
6. Zanzoni, A., Marchese, D., Agostini, F., Bolognesi, B., Cirillo, D., Botta-Orfila, M., Livi, C. M., Rodriguez-Mulero, S. & Tartaglia, G. G. (2013) Principles of self-organization in biological pathways: a hypothesis on the autogenous association of alpha-synuclein, *Nucleic Acids Research.* **41**, 9987-9998.
7. Breydo, L., Wu, J. W. & Uversky, V. N. (2012) Alpha-synuclein misfolding and Parkinson's disease, *Biochim Biophys Acta.* **1822**, 261-85.
8. Uversky, V. N. (2007) Neuropathology, biochemistry, and biophysics of alpha-synuclein aggregation, *J Neurochem.* **103**, 17-37.
9. Auluck, P. K., Caraveo, G. & Lindquist, S. (2010) alpha-Synuclein: membrane interactions and toxicity in Parkinson's disease, *Annu Rev Cell Dev Biol.* **26**, 211-33.
10. Kayed, R., Head, E., Thompson, J. L., McIntire, T. M., Milton, S. C., Cotman, C. W. & Glabe, C. G. (2003) Common structure of soluble amyloid oligomers implies common mechanism of pathogenesis, *Science.* **300**, 486-9.
11. Kayed, R., Sokolov, Y., Edmonds, B., McIntire, T. M., Milton, S. C., Hall, J. E. & Glabe, C. G. (2004) Permeabilization of lipid bilayers is a common conformation-dependent activity of soluble amyloid oligomers in protein misfolding diseases, *J Biol Chem.* **279**, 46363-6.
12. Jao, C. C., Hegde, B. G., Chen, J., Haworth, I. S. & Langen, R. (2008) Structure of membrane-bound alpha-synuclein from site-directed spin labeling and computational refinement, *Proc Natl Acad Sci U S A.* **105**, 19666-71.
13. Davidson, W. S., Jonas, A., Clayton, D. F. & George, J. M. (1998) Stabilization of alpha-synuclein secondary structure upon binding to synthetic membranes, *J Biol Chem.* **273**, 9443-9.

14. Rhoades, E., Ramlall, T. F., Webb, W. W. & Eliezer, D. (2006) Quantification of alpha-synuclein binding to lipid vesicles using fluorescence correlation spectroscopy, *Biophys J.* **90**, 4692-700.
15. Middleton, E. R. & Rhoades, E. (2010) Effects of curvature and composition on alpha-synuclein binding to lipid vesicles, *Biophys J.* **99**, 2279-88.
16. Shvadchak, V. V., Yushchenko, D. A., Pievo, R. & Jovin, T. M. (2011) The mode of alpha-synuclein binding to membranes depends on lipid composition and lipid to protein ratio, *FEBS Lett.* **585**, 3513-9.
17. Kjaer, L., Giehm, L., Heimburg, T. & Otzen, D. (2009) The influence of vesicle size and composition on alpha-synuclein structure and stability, *Biophys J.* **96**, 2857-70.
18. Pandey, A. P., Haque, F., Rochet, J. C. & Hovis, J. S. (2009) Clustering of alpha-synuclein on supported lipid bilayers: role of anionic lipid, protein, and divalent ion concentration, *Biophys J.* **96**, 540-51.
19. Stockl, M., Fischer, P., Wanker, E. & Herrmann, A. (2008) Alpha-synuclein selectively binds to anionic phospholipids embedded in liquid-disordered domains, *J Mol Biol.* **375**, 1394-404.
20. Danzer, K. M., Haasen, D., Karow, A. R., Moussaud, S., Habeck, M., Giese, A., Kretzschmar, H., Hengerer, B. & Kostka, M. (2007) Different species of alpha-synuclein oligomers induce calcium influx and seeding, *J Neurosci.* **27**, 9220-32.
21. Cappai, R., Leck, S. L., Tew, D. J., Williamson, N. A., Smith, D. P., Galatis, D., Sharples, R. A., Curtain, C. C., Ali, F. E., Cherny, R. A., Culvenor, J. G., Bottomley, S. P., Masters, C. L., Barnham, K. J. & Hill, A. F. (2005) Dopamine promotes alpha-synuclein aggregation into SDS-resistant soluble oligomers via a distinct folding pathway, *FASEB J.* **19**, 1377-9.
22. Lashuel, H. A., Petre, B. M., Wall, J., Simon, M., Nowak, R. J., Walz, T. & Lansbury, P. T., Jr. (2002) Alpha-synuclein, especially the Parkinson's disease-associated mutants, forms pore-like annular and tubular protofibrils, *J Mol Biol.* **322**, 1089-102.
23. van Rooijen, B. D., Claessens, M. M. & Subramaniam, V. (2009) Lipid bilayer disruption by oligomeric alpha-synuclein depends on bilayer charge and accessibility of the hydrophobic core, *Biochim Biophys Acta.* **1788**, 1271-8.
24. van Rooijen, B. D., Claessens, M. M., and Subramaniam, V. (2010) Membrane Permeabilization by Oligomeric a-Synuclein: In Search of the Mechanism, *PLoS ONE.* **5**.
25. Volles, M. J., Lee, S. J., Rochet, J. C., Shtilerman, M. D., Ding, T. T., Kessler, J. C. & Lansbury, P. T., Jr. (2001) Vesicle permeabilization by protofibrillar alpha-synuclein: implications for the pathogenesis and treatment of Parkinson's disease, *Biochemistry.* **40**, 7812-9.
26. Meratan, A. A., Ghasemi, A. & Nemat-Gorgani, M. (2011) Membrane integrity and amyloid cytotoxicity: a model study involving mitochondria and lysozyme fibrillation products, *J Mol Biol.* **409**, 826-38.
27. Nakamura, K., Nemani, V. M., Azarbal, F., Skibinski, G., Levy, J. M., Egami, K., Munishkina, L., Zhang, J., Gardner, B., Wakabayashi, J., Sesaki, H., Cheng, Y., Finkbeiner, S., Nussbaum, R. L., Masliah, E. & Edwards, R. H. (2011) Direct membrane association drives mitochondrial fission by the Parkinson disease-associated protein alpha-synuclein, *J Biol Chem.* **286**, 20710-26.
28. Yong-Kee, C. J., Sidorova, E., Hanif, A., Perera, G. & Nash, J. E. (2012) Mitochondrial dysfunction precedes other sub-cellular abnormalities in an in vitro model linked with cell death in Parkinson's disease, *Neurotox Res.* **21**, 185-94.
29. Ardail, D., Privat, J. P., Egret-Charlier, M., Levrat, C., Lerme, F. & Louisot, P. (1990) Mitochondrial contact sites. Lipid composition and dynamics, *J Biol Chem.* **265**, 18797-802.
30. Ramakrishnan, M., Jensen, P. H. & Marsh, D. (2003) Alpha-synuclein association with phosphatidylglycerol probed by lipid spin labels, *Biochemistry.* **42**, 12919-26.
31. Zigoneanu, I. G., Yang, Y. J., Krois, A. S., Haque, E. & Pielak, G. J. (2012) Interaction of alpha-synuclein with vesicles that mimic mitochondrial membranes, *Biochim Biophys Acta.* **1818**, 512-9.
32. Liu, G., Zhang, C., Yin, J., Li, X., Cheng, F., Li, Y., Yang, H., Ueda, K., Chan, P. & Yu, S. (2009) alpha-Synuclein is differentially expressed in mitochondria from different rat brain regions and dose-dependently down-regulates complex I activity, *Neurosci Lett.* **454**, 187-92.

33. Wen-Wei Li, R., J ing-Chun Guo, Hui-Min Ren, Xi-Liang Zha, Jie-Shi Cheng and Ding-Fang Cai (2007) Localization of a-synuclein to mitochondria within midbrain of mice, *NeuroReport.* **18**, 1543-1546.
34. Parihar, M. S., Parihar, A., Fujita, M., Hashimoto, M. & Ghafourifar, P. (2008) Mitochondrial association of alpha-synuclein causes oxidative stress, *Cell Mol Life Sci.* **65**, 1272-84.
35. Devi, L., Raghavendran, V., Prabhu, B. M., Avadhani, N. G. & Anandatheerthavarada, H. K. (2008) Mitochondrial import and accumulation of alpha-synuclein impair complex I in human dopaminergic neuronal cultures and Parkinson disease brain, *J Biol Chem.* **283**, 9089-100.
36. Devi, L. & Anandatheerthavarada, H. K. (2010) Mitochondrial trafficking of APP and alpha synuclein: Relevance to mitochondrial dysfunction in Alzheimer's and Parkinson's diseases, *Biochim Biophys Acta.* **1802**, 11-9.
37. Guardia-Laguarta, C., Area-Gomez, E., Rub, C., Liu, Y., Magrane, J., Becker, D., Voos, W., Schon, E. A. & Przedborski, S. (2014) alpha-Synuclein is localized to mitochondria-associated ER membranes, *J Neurosci.* **34**, 249-59.
38. Fauvet, B., Fares, M. B., Samuel, F., Dikiy, I., Tandon, A., Eliezer, D. & Lashuel, H. A. (2012) Characterization of semisynthetic and naturally Nalpha-acetylated alpha-synuclein in vitro and in intact cells: implications for aggregation and cellular properties of alpha-synuclein, *J Biol Chem.* **287**, 28243-62.
39. Gitler, A. D., Bevis, B. J., Shorter, J., Strathearn, K. E., Hamamichi, S., Su, L. J., Caldwell, K. A., Caldwell, G. A., Rochet, J. C., McCaffery, J. M., Barlowe, C. & Lindquist, S. (2008) The Parkinson's disease protein alpha-synuclein disrupts cellular Rab homeostasis, *Proc Natl Acad Sci U S A.* **105**, 145-50.
40. Fiske, M., White, M., Valtierra, S., Herrera, S., Solvang, K., Konnikova, A. & Debburman, S. (2011) Familial Parkinson's Disease Mutant E46K alpha-Synuclein Localizes to Membranous Structures, Forms Aggregates, and Induces Toxicity in Yeast Models, *ISRN Neurol.* **2011**, 521847.
41. Pacheco, C., Aguayo, L. G. & Opazo, C. (2012) An extracellular mechanism that can explain the neurotoxic effects of alpha-synuclein aggregates in the brain, *Front Physiol.* **3**, 297.
42. Jo, E., McLaurin, J., Yip, C. M., St George-Hyslop, P. & Fraser, P. E. (2000) alpha-Synuclein membrane interactions and lipid specificity, *J Biol Chem.* **275**, 34328-34.
43. van Rooijen, B. D., Claessens, M. M. & Subramaniam, V. (2008) Membrane binding of oligomeric alpha-synuclein depends on bilayer charge and packing, *FEBS Lett.* **582**, 3788-92.
44. Zhu, M., Li, J. & Fink, A. L. (2003) The association of alpha-synuclein with membranes affects bilayer structure, stability, and fibril formation, *J Biol Chem.* **278**, 40186-97.
45. Wang, G. F., Li, C. & Pielak, G. J. (2010) 19F NMR studies of alpha-synuclein-membrane interactions, *Protein Sci.* **19**, 1686-91.
46. Zigoneanu, I. G., Yang, Y. J., Krois, A. S., Haque, E. & Pielak, G. J. (2012) Interaction of alpha-synuclein with vesicles that mimic mitochondrial membranes in *Biochim Biophys Acta* pp. 512-9
47. Pfefferkorn, C. M. & Lee, J. C. (2010) Tryptophan probes at the alpha-synuclein and membrane interface, *J Phys Chem B.* **114**, 4615-22.
48. Shvadchak, V. V., Falomir-Lockhart, L. J., Yushchenko, D. A. & Jovin, T. M. (2011) Specificity and kinetics of alpha-synuclein binding to model membranes determined with fluorescent excited state intramolecular proton transfer (ESIPT) probe, *J Biol Chem.* **286**, 13023-32.
49. Schwiering, M. & Hellmann, N. (2012) Validation of liposomal lipid composition by thin-layer chromatography, *J Liposome Res.* **22**, 279-84.
50. Chandra, S., Chen, X., Rizo, J., Jahn, R. & Sudhof, T. C. (2003) A broken alpha -helix in folded alpha -Synuclein, *J Biol Chem.* **278**, 15313-8.
51. Bartels, T., Ahlstrom, L. S., Leftin, A., Kamp, F., Haass, C., Brown, M. F. & Beyer, K. (2010) The N-terminus of the intrinsically disordered protein alpha-synuclein triggers membrane binding and helix folding, *Biophys J.* **99**, 2116-24.

52. Volles, M. & Lansbury, P. (2002) Vesicle permeabilization by protofibrillar alpha-synuclein is sensitive to Parkinson's disease-linked mutations and occurs by a pore-like mechanism, *Biochemistry.* **41**, 4595 - 4602.
53. Maherani, B., Arab-Tehrany, E., Kheirolomoom, A., Geny, D. & Linder, M. (2013) Calcein release behavior from liposomal bilayer; influence of physicochemical/mechanical/structural properties of lipids, *Biochimie.* **95**, 2018-2033.
54. Shimanouchi, T., Ishii, H., Yoshimoto, N., Umakoshi, H. & Kuboi, R. (2009) Calcein permeation across phosphatidylcholine bilayer membrane: effects of membrane fluidity, liposome size, and immobilization, *Colloids Surf B Biointerfaces.* **73**, 156-60.
55. Ouberai, M. M., Wang, J., Swann, M. J., Galvagnion, C., Guilliams, T., Dobson, C. M. & Welland, M. E. (2013) alpha-Synuclein senses lipid packing defects and induces lateral expansion of lipids leading to membrane remodeling, *J Biol Chem.* **288**, 20883-95.
56. Leftin, A., Job, C., Beyer, K. & Brown, M. F. (2013) Solid-State 13C NMR Reveals Annealing of Raft-Like Membranes Containing Cholesterol by the Intrinsically Disordered Protein α-Synuclein, *J Mol Biol.* **425**, 2973-2987.
57. Fantini, J. & Yahi, N. (2013) The driving force of alpha-synuclein insertion and amyloid channel formation in the plasma membrane of neural cells: key role of ganglioside- and cholesterol-binding domains, *Adv Exp Med Biol.* **991**, 15-26.
58. Fantini, J., Carlus, D. & Yahi, N. (2011) The fusogenic tilted peptide (67-78) of alpha-synuclein is a cholesterol binding domain, *Biochim Biophys Acta.* **1808**, 2343-51.
59. Brender, J. R., Lee, E. L., Hartman, K., Wong, P. T., Ramamoorthy, A., Steel, D. G. & Gafni, A. (2011) Biphasic effects of insulin on islet amyloid polypeptide membrane disruption, *Biophys J.* **100**, 685-92.
60. Zijlstra, N., Blum, C., Segers-Nolten, I. M., Claessens, M. M. & Subramaniam, V. (2012) Molecular composition of sub-stoichiometrically labeled alpha-synuclein oligomers determined by single-molecule photobleaching, *Angew Chem Int Ed Engl.* **51**, 8821-4.
61. Camilleri, A., Zarb, C., Caruana, M., Ostermeier, U., Ghio, S., Hogen, T., Schmidt, F., Giese, A. & Vassallo, N. (2013) Mitochondrial membrane permeabilisation by amyloid aggregates and protection by polyphenols, *Biochim Biophys Acta.* **1828**, 2532-43.
62. van Raaij, M. E., Segers-Nolten, I. M. J. & Subramaniam, V. (2006) Quantitative Morphological Analysis Reveals Ultrastructural Diversity of Amyloid Fibrils from α-Synuclein Mutants, *Biophys J.* **91**, L96-L98.
63. Pace, C. N., Vajdos, F., Fee, L., Grimsley, G. & Gray, T. (1995) How to measure and predict the molar absorption coefficient of a protein, *Protein Sci.* **4**, 2411-23.
64. van Meer, G., Voelker, D. R. & Feigenson, G. W. (2008) Membrane lipids: where they are and how they behave, *Nat Rev Mol Cell Biol.* **9**, 112-124.
65. Angelova, M. I. & Dimitrov, D. S. (1986) Liposome Electroformation, *Faraday Disc Chem Soc.* **81**, 303-311.
66. Barrow, C. J., Yasuda, A., Kenny, P. T. & Zagorski, M. G. (1992) Solution conformations and aggregational properties of synthetic amyloid beta-peptides of Alzheimer's disease, *J Mol Biol.* **225**, 1075-93.
67. Chen, Y. H., Yang, J. T. & Chau, K. H. (1974) Determination of the Helix and beta Form of Proteins in Aqueous Solution by Circular Dichroism, *Biochemistry.* **13**, 3350-9.
68. Scholtz, J. M., Qian, H., York, E. J., Stewart, J. M. & Baldwin, R. L. (1991) Parameters of Helix-Coil Transition Theory for Alanine-Based Peptides of Varying Chain Lengths in Water, *Biopolymers.* **31**, 1463-1470.

TABLES

Table 1: Fitting parameters for oligomer-induced calcein leakage from CL:POPE:POPC vesicles [a, b].

Concentration	*A*	*B*	*C*	k_1	k_2	k_3
µM				h^{-1}	h^{-1}	h^{-1}
4	6.4±0.17	7.8±0.13	86	10.87±0.59	0.47±0.02	0.004
3	6.33±0.14	7.39±0.12	86	10.15±0.47	0.45±0.02	0.004
2	5.8±0.1	7.5±0.08	85.5	12.59±0.47	0.47±0.012	0.004
1	2.87±0.06	4.79±0.07	92	10.58±0.48	0.34±0.01	0.002
0.5	2.69±0.04	2.69±0.07	94.03	13.88±0.47	0.31±0.01	0.001
0.25	2.52±0.04	1.31±0.03	96.4	13.28±0.4	0.37±0.03	<0.001

[a] Fits were determined using $y = A\times\left(1-e^{-k_1\times t}\right)+B\times\left(1-e^{-k_2\times t}\right)+C\times\left(1-e^{-k_3\times t}\right)+y_0$, *A and B*, preexponential factors associated with oligomer-induced leakage, k_1 and k_2, rate constant of oligomer-induced leakage; *C*, preexponental factor of bare membrane leakage, k_3, rate constant bare vesicle leakage, y_0, the offset.
[b] We present calcein release kinetics measured for 6 different oligomer concentrations: 4 µM, 3 µM, 2 µM, 1 µM, 0.5 µM 0.25 µM. At least three exponentials were necessary for adequate fits of our data.

FIGURE LEGENDS

Figure 1: Representative confocal microscopy images of DOPE-Rhodamine labeled GUVs (red channel) and αS wt-140C-A488 monomers (green channel). Binding of αS monomers to A) DOPG, B) CL:POPE:POPC (4:3:5), C) Brain PS:brain PE:cholesterol (2:5:3) membranes is depicted. D) Semiquantitative analysis of fluorescently labeled αS bound to vesicles (n = 15). The error bars represent standard deviation. The scale bars indicate 5 μm. The same experimental settings (master gain, digital offset and laser power) were used for all images.

Figure 2: Circular dichroism measurements of conformational changes of αS monomers (· · ·) upon binding to membranes. A) Binding of αS to DOPG (− · −), CL:POPE:POPC (····) and brain PS:brain PE:ch (− −) vesicles showed increase of α-helical content. There is no change in α-helical content of αS monomers bound to brain PS:brain PE:ch vesicles with time when comparing CD spectra 10 minutes (−−)after binding or after 20h of incubation (−). B) Percentage of α-helix formed for αS monomers bound to vesicles with the lipid compositions tested above. Data are the average of 3 different measurements. Error bars represent standard deviations.

Figure 3: Representative confocal microscopy images of DOPE-Rhodamine labeled GUVs (red channel) and αS wt-140C-A488 oligomers (green channel). Binding of αS oligomers to A) DOPG, B) CL:POPE:POPC, C) brain PS:brain PE:ch vesicles is depicted. D) Semiquantitative analysis of fluorescently labeled oligomers bound to vesicles (n = 15). The error bars represent standard deviation. The scale bars indicate 5 μm. The same experimental settings (master gain, digital offset and laser power) were used for all images.

Figure 4: Circular dichroism measurements of conformational changes of αS oligomers upon binding to membranes. Oligomers partially adopted α-helical structure upon addition of SUVs. No difference in changes of protein conformation was observed after 20h for αS oligomers binding to brain PS:brain PE:ch vesicles. Legend: αS oligomers (· · ·), DOPG (− · −), CL:POPE:POPC (····) and brain PS:brain PE:ch after 10 minutes (− −) and 20 h of incubation (−).

Figure 5: Dye release kinetics from vesicles of different lipid composition after addition of αS oligomers. A) with DOPG vesicles 1 μM oligomers showed almost complete leakage and fast kinetics which reached a plateau after 12 minutes. B) CL:POPE:POPC vesicles did not result in comparable leakage after 18 hours even with 4 μM oligomer concentration. C) Oligomers did not induce appreciable leakage in brain PS:brain PE:ch model membranes even on a long time scale. Legend: 4 μM oligomers (− − −), 1 μM oligomers (· · ·), 0.5 μM oligomers (− · −) and lipids alone (⋯).

Figure 6: Typical DLS graph for CL:POPE:POPC LUVs before and after addition of oligomers. Parameters from DLS measurements are described as volume of particles (%) as a function of size (nm) ($F\ (size, nm) = volume\ of\ vesicles, \%$) for vesicles alone (CL:POPE:POPC (−)) and vesicles + oligomers (− − −). Changes in diameter between membranes (144.1±6.0) and membranes after addition of oligomers (177.8±15.1) are ~ 30 nm for CL:POPE:POPC membranes. Peak width changes were ~ 12 nm; peak width of vesicles alone is 50.2±6.5 nm and peak width after 18h of incubation with oligomers is 62.6±4.5 nm.

Figure 7: Oligomer-induced leakage kinetics from vesicles of different lipid composition: DOPG:DOPC (1:2, black circles), DOPG:DOPC (1:4, grey triangles), DOPG:DOPC:ch (2:5:3, blue pentagons) and DOPG:DOPC:ch (4:3:5, red circles). Oligomers at 1 μM (equivalent monomer) concentration were incubated with these lipid membranes for 18 h. Oligomer-induced leakage was less than 5%, which is comparable to the data observed with our plasma inner leaflet membrane mimics.

FIGURES

Figure 1

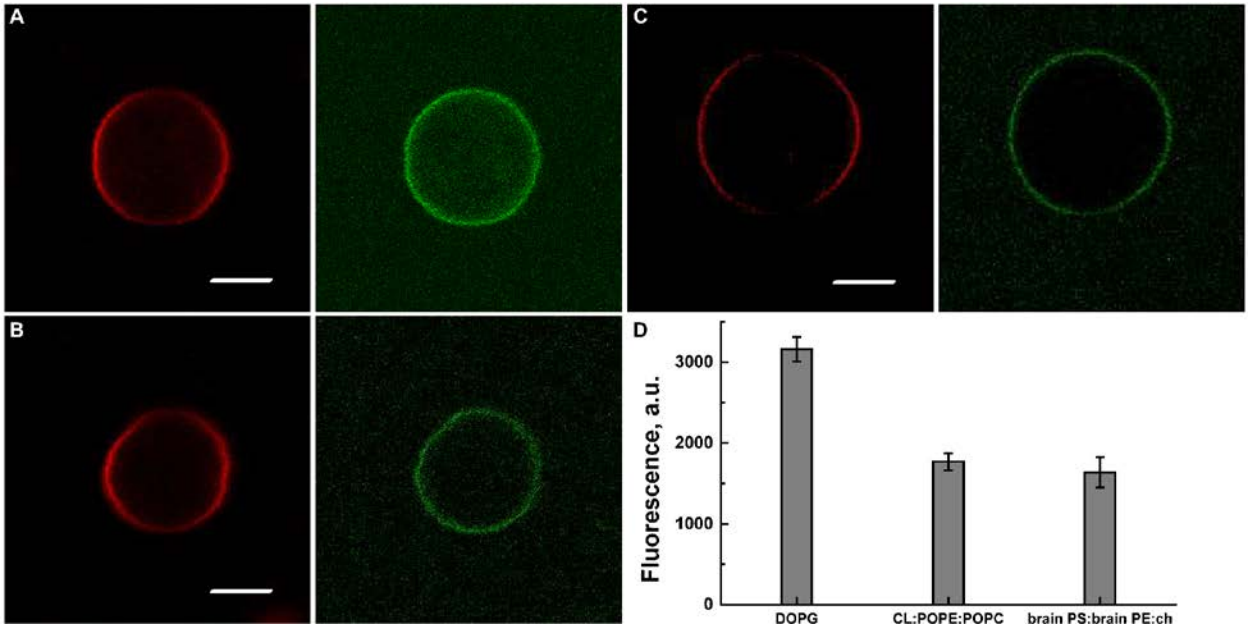

Figure 2

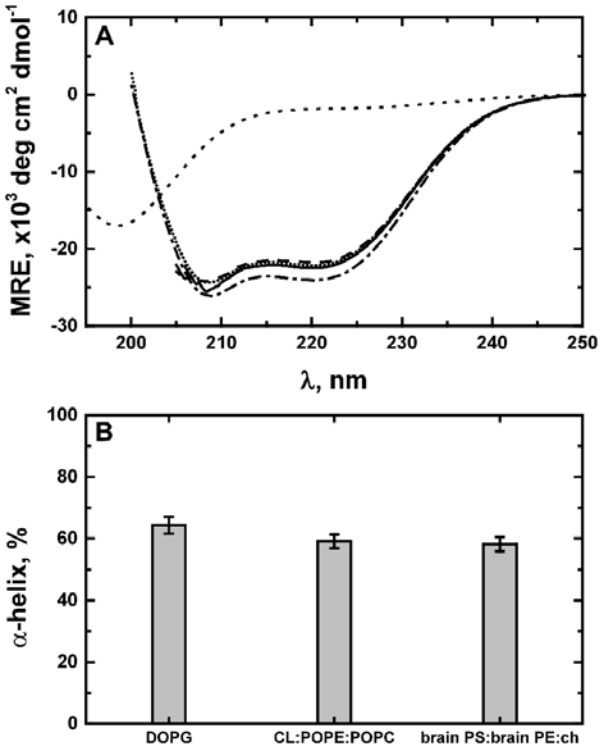
A
MRE, x10^3 deg cm^2 dmol^{-1}
10
0
-10
-20
-30
200
210
220
230
240
250
λ, nm
B
α-helix, %
100
80
60
40
20
0
DOPG
CL:POPE:POPC
brain PS:brain PE:ch

Figure 3

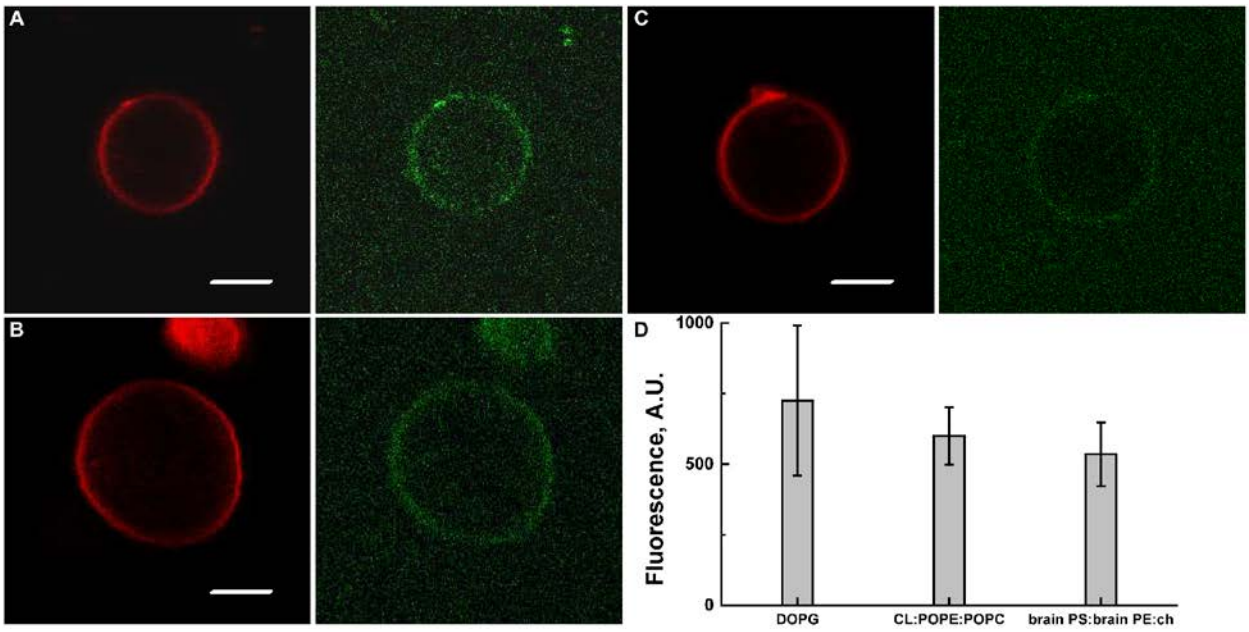
A
B
C
D
1000
500
0
Fluorescence, A.U.
DOPG
CL:POPE:POPC
brain PS:brain PE:ch

Figure 4

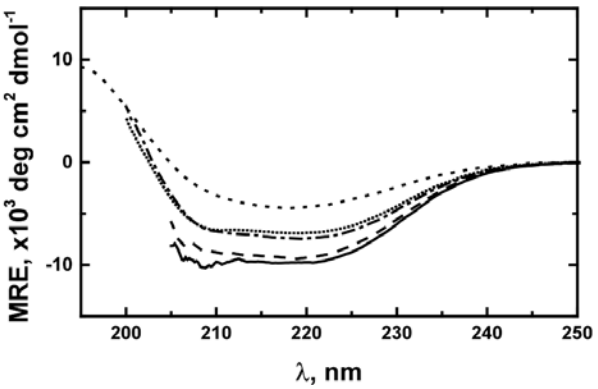

Figure 5

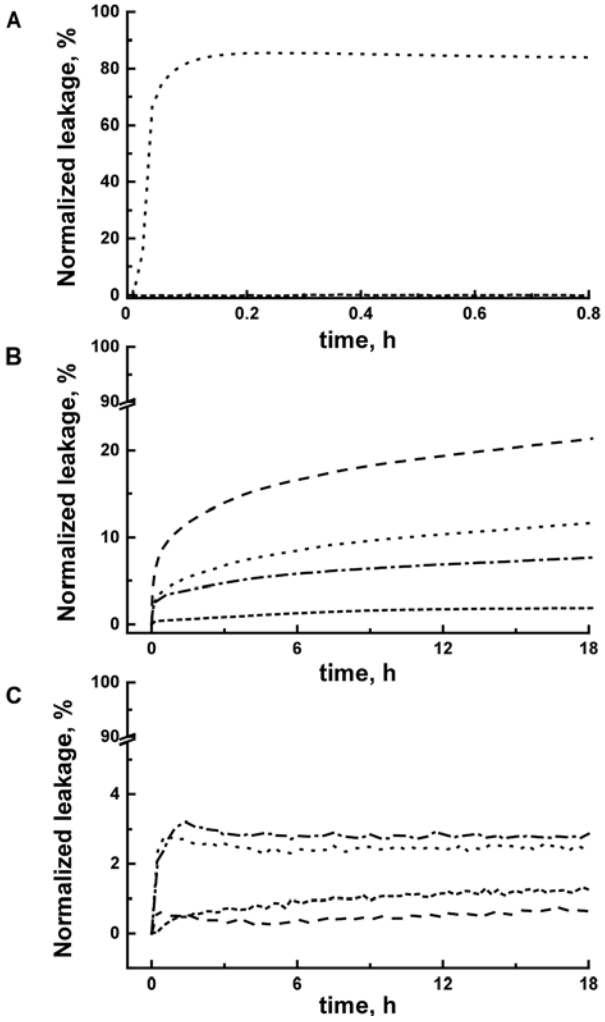
A
Normalized leakage, %
100
80
60
40
20
0
0
0.2
0.4
0.6
0.8
time, h
B
Normalized leakage, %
100
90
20
10
0
0
6
12
18
time, h
C
Normalized leakage, %
100
90
4
2
0
0
6
12
18
time, h

Figure 6

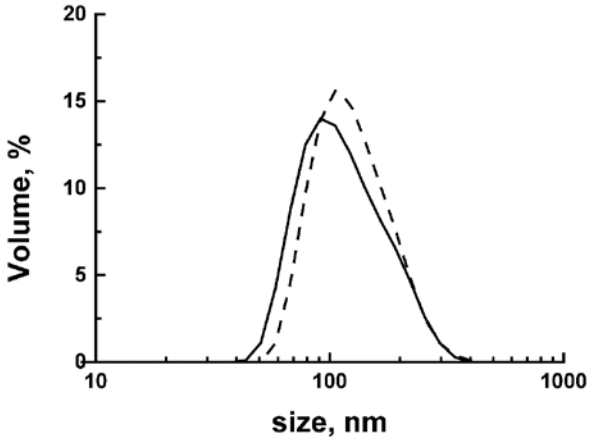

Figure 7

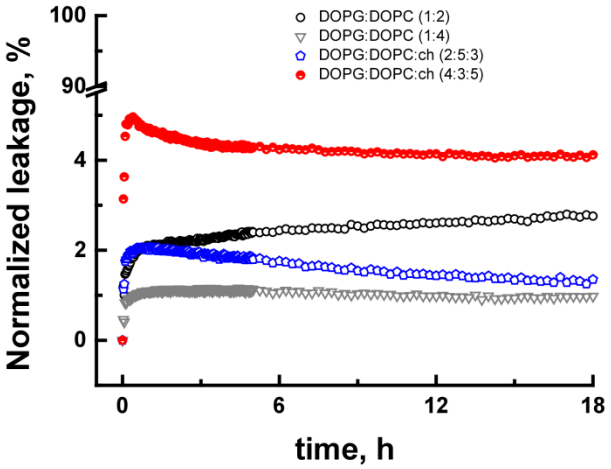
DOPG:DOPC (1:2)
DOPG:DOPC (1:4)
DOPG:DOPC:ch (2:5:3)
DOPG:DOPC:ch (4:3:5)
Normalized leakage, %
100
90
4
2
0
0
6
12
18
time, h

Alpha-synuclein Oligomers Distinctively Permeabilize Complex Model Membranes*

Anja N.D. Stefanovic[1], Martin T. Stöckl[1,2], Mireille M. A. E. Claessens[1], Vinod Subramaniam[1,3]

[1] Nanobiophysics group, MIRA Institute for Biomedical Technology and Technical Medicine and MESA+ Institute for Nanotechnology, University of Twente, PO Box 217, 7500AE, The Netherlands

[2] present address: Bioimaging Center, University Konstanz, PO Box 604, Universitätsstraße 10, 78457 Konstanz, Germany

[3] present address: FOM Institute AMOLF, Science Park 104, 1098XG Amsterdam, The Netherlands

Running title: α-synuclein oligomer-complex membrane interactions

Correspondence: Vinod Subramaniam, FOM Institute AMOLF & University of Twente, Science Park 104, 1098 XG Amsterdam, The Netherlands, Tel.: +31 20 7547100; Fax: +31 20 754 7290; Email: subramaniam@amolf.nl

SUPPORTING INFORMATION

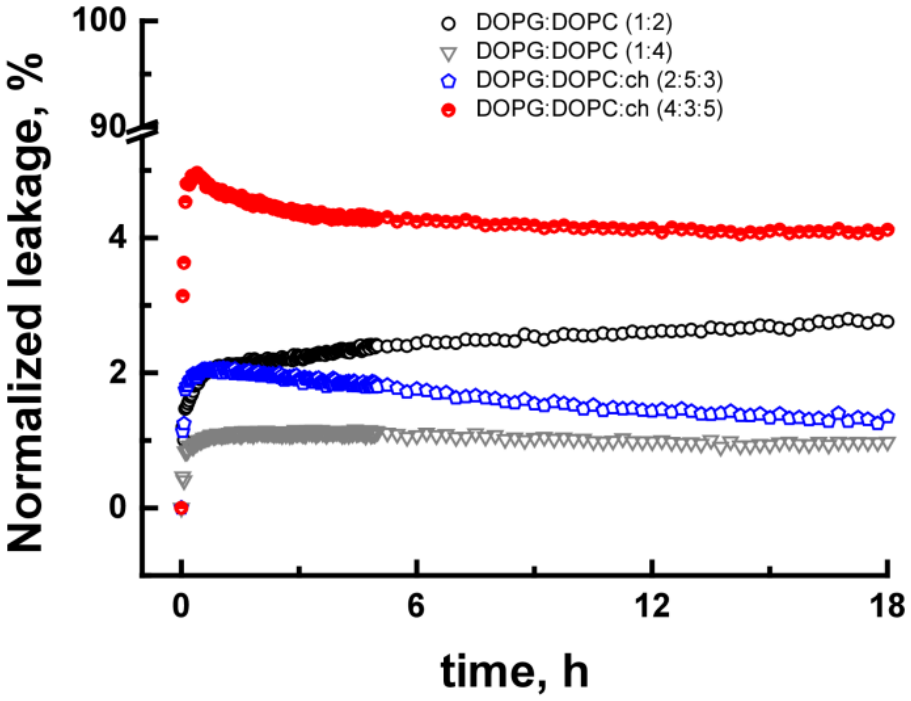

Figure S1: *Oligomer-induced leakage kinetics from vesicles of different lipid composition: DOPG:DOPC (1:2, black circles), DOPG:DOPC (1:4, grey triangles), DOPG:DOPC:ch (2:5:3, blue pentagons) and DOPG:DOPC:ch (4:3:5, red circles). Oligomers at 1 μM (equivalent monomer) concentration were incubated with these lipid membranes for 18 h. Oligomer-induced leakage was less than 5% which is comparable to the data observed with our plasma inner leaflet membrane mimics.*